Zitterbewegung effect in spin-orbit-coupled spin-1 ultracold atoms

Yi-Cai Zhang,[1] Shu-Wei Song,[1] Chao-Fei Liu,[1,2] and Wu-Ming Liu[1]

[1]*Beijing National Laboratory for Condensed Matter Physics, Institute of Physics, Chinese Academy of Sciences, Beijing 100190, China*

[2]*School of Science, Jiangxi University of Science and Technology, Ganzhou 341000, China*

(Received 25 November 2012; published 15 February 2013)

The *Zitterbewegung* effect in spin-orbit-coupled spin-1 cold atoms is investigated in the presence of the Zeeman field and a harmonic trap. It is shown that the Zeeman field and the harmonic trap have significant effect on the *Zitterbewegung* oscillatory behaviors. The external Zeeman field could suppress or enhance the *Zitterbewegung* amplitude and change the frequencies of oscillation. A much slowly damping *Zitterbewegung* oscillation can be achieved by adjusting both the linear and the quadratic Zeeman fields. Multifrequency *Zitterbewegung* oscillation can be induced by the applied Zeeman field. In the presence of the harmonic trap, the subpackets corresponding to different eigenenergies would always keep coherent, resulting in the persistent *Zitterbewegung* oscillations. The *Zitterbewegung* oscillation would display very complicated and irregular oscillation characteristics due to the coexistence of different frequencies of the *Zitterbewegung* oscillation. Furthermore, numerical results show that the *Zitterbewegung* effect is robust even in the presence of interaction between atoms.

DOI: 10.1103/PhysRevA.87.023612 PACS number(s): 03.75.Mn, 67.85.Fg, 05.30.Jp

I. INTRODUCTION

The *Zitterbewegung* (ZB) effect, which is characterized by high-frequency oscillations (trembling motion) for Dirac electrons was first predicted by Schrödinger [1]. The ZB effect is purely a relativistic phenomenon and originates from the interference between the positive and negative energy states of the electron. The experimental observation of the electron ZB has not been realized due to its high frequency (the order of $\hbar\omega = 2m_ec^2 \sim 1$ MeV) and small oscillatory amplitude (the order of Compton wavelength of electron $\hbar/m_ec \sim 10^{-12}$ m). However, it is shown that there exist ZB-like effects in graphene [2,3], superconductors [4], photonic crystal [5], single trapped ion [6,7], and semiconductor quantum wells [8,9]. Hence, the ZB-like effect has attracted great attention recently, both theoretically and experimentally, in various physics fields [10–13].

Most of these studies of the ZB effect are based on the Dirac-like equation with spin-orbit coupling interaction. The spin-orbit coupling interaction plays an essential role in a lot of interesting phenomena, such as quantum spin Hall effects, topological insulator, exotic superconductivity, or superfluidity, etc. In recent years, the spin-orbit coupling interaction in cold atoms have attracted great attentions both experimentally and theoretically. The spin-orbit coupling in two-component atoms has been created experimentally with Raman laser beams [14–17]. The proposal to realize spin-orbit coupling for three-component atoms has been put forward in Ref. [18]. Using the so-called tetrapod setup scheme and two pairs of counterpropagating laser beams, the spin-orbit coupling in spin-1 atoms could be realized in alkali-metal atoms. The resulting gauge potential is proportional to the projection of angular momentum operator of spin-1 atoms along xy plane. The ground states of the spin-orbit-coupled Bose-Einstein condensate (BEC) have been extensively studied theoretically. For example, in the case of strong coupling and the weak harmonic trap, the spin-orbit coupling would result in a nontrivial ground state in BEC, such as a plane wave phase or standing wave phase, which depends on interaction between atoms [19–21]. For the strong coupling and the strong harmonic trap, the half-quantum vortex phase or vortex lattice phase develops [22–26].

The length and energy scales can be well controlled in cold atoms. Thus, it is possible to observe the ZB-like oscillation in cold-atom experiments. Recently, there were proposals to simulate the ZB effect by using spin-orbit-coupled ultracold atoms [27–30], wherein most authors focus on the ZB effect of two-component atoms with spin-orbit coupling in free space. Thus, the quasimomenta is a good quantum number and the Hamiltonian can be diagonalized within the momentum space. By using the Gaussian packet as the initial state, it is shown that the amplitude of the ZB oscillation deceases with time and the ZB phenomenon has a transient characteristic. On the other hand, ZB-like phenomena are fairly common characteristics for multilevel systems [31]. It is worthwhile to notice that the ZB oscillation of two-component atoms has only one single frequency. Compared with the two-component atoms, a multifrequency ZB oscillation may appear due to the richer energy spectrum structure in the three-component atoms. Moreover, as shown in the present paper, the richer energy spectrum structure in three-component atoms provides more possibilities to stabilize the ZB oscillation of cold atoms by utilizing the Zeeman field. The effects induced by the trap on the ZB oscillations also need to be clarified.

In the present paper, we investigate the characteristics of the multifrequency oscillation induced by Zeeman field and the persistent oscillations in the presence of the external harmonic trap in the spin-1 ultracold atoms. In Sec. II, we introduce the general Hamiltonian of spin-1 atoms with spin-orbit coupling and then focus on the ZB oscillatory characteristics in the Zeeman fields. In Sec. III, the ZB oscillatory characteristics in harmonic trap are investigated. In Sec. IV, the effect of the interaction between atoms on the ZB oscillation is considered. A summary is presented in Sec. V.

II. *ZITTERBEWEGUNG* EFFECT IN ZEEMAN FIELDS

The two-dimensional Hamiltonian of the spin-orbit-coupled spin-1 atoms in the presence of the external Zeeman

field and harmonic trap is [19]

$$\begin{aligned} H &= T + V_{\rm trap} + V_{\rm SO} + V_Z + H_{\rm int}, \\ T &= \int d\vec{r}\Psi^\dagger \frac{p_x^2 + p_y^2}{2M}\Psi, \\ V_{\rm trap} &= \int d\vec{r}\Psi^\dagger \frac{M\omega^2(x^2+y^2)}{2}\Psi, \\ V_{\rm SO} &= \int d\vec{r}\Psi^\dagger[\gamma p_x F_x + \gamma p_y F_y]\Psi, \\ V_Z &= \int d\vec{r}\Psi^\dagger\left[pF_z + qF_z^2\right]\Psi, \\ H_{\rm int} &= \int d\vec{r}\left[\frac{c_0}{2}\hat{n}^2 + \frac{c_2}{2}\mathbf{F}^2\right], \end{aligned} \tag{1}$$

where T, $V_{\rm trap}$, $V_{\rm SO}$, V_Z, $H_{\rm int}$ are the kinetic energy, the harmonic potential, the spin-orbit coupling interaction, the effective Zeeman shift, and the interaction between atoms, respectively. The spin-orbit coupling strength $\gamma = 2\pi\hbar\sin(\theta/2)/(M\lambda)$, the effective Zeeman parameters $p = \hbar(\Delta\omega_l - \omega_Z)$ and $q = (g\mu_B B)^2/\Delta E_{hf}$, where θ is the angle between two Raman beams, and λ is the wavelength of the laser beam, $\Delta\omega_l$ is the frequency difference between Raman lasers, $\omega_Z = |g|\mu_B B$ is the liner Zeeman shift, g is the Landé g factor, $\mu_B = e\hbar/2m_e$ is the Bohr magneton and ΔE_{hf} the hyperfine energy splitting [32]. The parameters (γ, p, and q) in the Hamiltonian is tunable in cold atomic experiments [14–17]. $\Psi = (\Psi_1, \Psi_0, \Psi_{-1})^T$, $\hat{n} = \hat{n}_1 + \hat{n}_0 + \hat{n}_{-1}$, $\mathbf{F} = \Psi_\alpha^\dagger \vec{F}_{\alpha\beta}\Psi_\beta$, $c_0 = 4\pi\hbar^2(a_0 + 2a_2)/3m$, and $c_2 = 4\pi\hbar^2(a_2 - a_0)/3$ are the field operator, the number density operator, the angular momentum operator, the spin-independent interaction parameter, and the spin-dependent interaction parameter, respectively. a_0 and a_2 are the s-wave scattering lengths corresponding to the total spin of the two colliding bosons 0 and 2, respectively.

The Pauli spin matrices for spin-1 atoms are given by

$$F_x = \begin{pmatrix} 0 & \frac{1}{\sqrt{2}} & 0 \\ \frac{1}{\sqrt{2}} & 0 & \frac{1}{\sqrt{2}} \\ 0 & \frac{1}{\sqrt{2}} & 0 \end{pmatrix}, \quad F_y = \begin{pmatrix} 0 & \frac{-i}{\sqrt{2}} & 0 \\ \frac{i}{\sqrt{2}} & 0 & \frac{-i}{\sqrt{2}} \\ 0 & \frac{i}{\sqrt{2}} & 0 \end{pmatrix},$$

$$F_z = \begin{pmatrix} 1 & 0 & 0 \\ 0 & 0 & 0 \\ 0 & 0 & -1 \end{pmatrix}.$$

Without the external harmonic trap and interaction, the Hamiltonian can be diagonalized in the momentum space as

$$H' = \begin{pmatrix} \omega_1 & 0 & 0 \\ 0 & \omega_2 & 0 \\ 0 & 0 & \omega_3 \end{pmatrix}, \tag{2}$$

where $\omega_1 = (p_x^2 + p_y^2)/2m + n\cos u - b/3$, $\omega_2 = (p_x^2 + p_y^2)/2m + n\cos(u + 4\pi/3) - b/3$, $\omega_3 = (p_x^2 + p_y^2)/2m + n\cos(u + 2\pi/3) - b/3$ are roots of eigenequation $\mathrm{Det}(\omega I - H) = 0$. The corresponding eigenvectors are

$$|\alpha_i\rangle = \frac{1}{n_i}\begin{pmatrix} -(p_x^2 + p_y^2) + 2\omega_i(p - q + \omega_i) \\ \sqrt{2}(p - q + \omega_i)(p_x + ip_y) \\ (p_x + ip_y)^2 \end{pmatrix}, \tag{3}$$

where n_i is the normalization coefficient, $n = \sqrt{-4p_1/3}$, $u = \arccos[-q_1(-p_1/3)^{-3/2}/2]/3$, $p_1 = c - b^2/3$, $q_1 = d - bc/3 + 2b^3/27$, $b = -2q$, $c = -(p_x^2 + p_y^2) + q^2 - p^2$, $d = (p_x^2 + p_y^2)q$, respectively. In general, they are the functions of the momentum (p_x, p_y) and Zeeman parameters (p, q).

The position operator in the Heisenberg picture is [31]

$$\vec{r}(t) = \vec{r}(0) + \sum_k Z_{k;k} + t\sum_k \vec{V}_k Q_k + \sum_{k,l\neq m} e^{i\frac{\omega_{kl}t}{\hbar}}\vec{Z}_{k;l}, \tag{4}$$

where $\vec{V}_k = \frac{\partial\omega_k}{\partial\vec{p}}$, $Q_k = |\alpha_k\rangle\langle\alpha_k|$ are the group velocity and the projection operator, respectively. k, l denote the energy branch ω_1, ω_2, ω_3 and $\omega_{kl} = \omega_k - \omega_l$ is the eigenenergy difference. $Z_{k;l} = iQ_k\frac{\partial Q_l}{\partial\vec{p}}$ is the so-called *ZB amplitudes* (see Ref. [31]). The first and second terms are constants in Eq. (4). The third term is the uniform motion and the fourth one corresponds to the ZB oscillation. As shown in the fourth term, the position operator usually undergoes a multifrequency oscillation. We calculate the average value of position by using an initial wave function of Gaussian density distribution:

$$|g\rangle = \frac{1}{\sqrt{\pi\delta^2}}e^{-\frac{x^2+y^2}{2\delta^2}}e^{\frac{ik_0x}{\hbar}}\begin{pmatrix} 1 \\ 0 \\ 0 \end{pmatrix}. \tag{5}$$

The wave function expressed in momentum space is

$$|g\rangle = \sqrt{\frac{\delta^2}{\pi}}e^{-\frac{\delta^2}{2\hbar^2}[(p_x-k_0)^2+p_y^2]}\begin{pmatrix} 1 \\ 0 \\ 0 \end{pmatrix}, \tag{6}$$

where δ and k_0 are the width and the average momentum of the wave packet. The mean value of position is $\langle\vec{r}(t)\rangle = \langle g|\vec{r}(t)|g\rangle$.

From Eq. (4), we can find that the kinetic energy of Hamiltonian does not contribute to the ZB oscillation. Therefore, during the discussion of the ZB in this section, the kinetic energy part is neglected. In this section, we take the reduced Plank constant $\hbar$, the spin-orbit coupling strength γ, and the wave-packet width δ as independent fundamental units. The other derived physical quantities, such as time, momentum, and energy are measured by δ/γ, $\hbar/\delta$, and $\gamma\hbar/\delta$, respectively.

We explore the following four cases according to the applied Zeeman field.

A. The *Zitterbewegung* under zero Zeeman field ($p = 0$ and $q = 0$)

Considering the initial wave packet (5), only the matrix element of $(y(t))_{1,1}$ has contribution to the the oscillation part of the y component of the position operator. In the Heisenberg picture, it takes the form

$$y(t)_{1,1} = \frac{p_x}{p_x^2 + p_y^2}\cos\left(t\sqrt{p_x^2 + p_y^2}\right). \tag{7}$$

Substituting the initial state, we calculate the mean value of the oscillatory part of y

$$\begin{aligned} \langle y(t)\rangle &= \int_{-\infty}^{\infty}\int_{-\infty}^{\infty} d\vec{p}\frac{1}{\pi}\frac{p_x\cos\left(t\sqrt{p_x^2 + p_y^2}\right)e^{-[(p_x-k_0)^2+p_y^2]}}{p_x^2 + p_y^2} \\ &= 2e^{-k_0^2}\mathrm{Re}\left[\int_0^\infty d\rho e^{-\rho^2+it\rho}I_1(2k_0\rho)\right], \end{aligned} \tag{8}$$

where $\rho = \sqrt{p_x^2 + p_y^2}$ and $I_1(x)$ are variable of integration and the modified Bessel function of first order, respectively. In order to capture qualitative behaviors of ZB oscillation, we assume $k_0 \gg 1$, and the asymptotic formula $I_1(x) \approx e^x/\sqrt{2\pi x}$ can be used [33]. The integral $\int_0^\infty d\rho e^{(-\rho^2+It\rho+2k_0\rho)}/\sqrt{2k_0\rho}$ can be evaluated using the method of steepest descents

$$\langle y(t)\rangle \approx \frac{e^{-\frac{t^2}{4}}}{\left(k_0^4 + \frac{k_0^2 t^2}{4}\right)^{\frac{1}{4}}} \cos\left(k_0 t - \frac{\theta}{2}\right), \tag{9}$$

where $\theta = \arctan(\frac{t}{2k_0})$ denotes a phase shift of ZB oscillation.

From Eq. (9), it is shown that in the case of $k_0 \gg 1$, the average position in the the direction perpendicular to the average momentum k_0 undergos a damping oscillation with a single frequency. There are two factors which result in the damping. One is the exponentially decreasing term $e^{-\frac{t^2}{4}}$, which originates from the increasing spatial separation between the subpackets corresponding to the higher and lower eigenenergy branches [34]. Because the overlap between the subpackets gets smaller and smaller with time, the amplitude of the oscillation gets smaller and smaller. We can identify the nonvanishing relative group velocity between the subpackets corresponding to different energy branches at the average momentum $v = \partial_{p_x}\omega_{12}|_{k_0} = 1$. It is anticipated that, when the relative group velocity gets smaller, the damping would be suppressed. The other one is the term $1/(k_0^4 + \frac{k_0^2 t^2}{4})^{\frac{1}{4}}$, which results in a much slower damping compared with the exponentially decreasing term. In the case of $k_0 \gg 1$, the exponentially decreasing term dominates the whole damping trend before the disappearing of the ZB. Although there exists a phase shift θ during the damping process of ZB oscillation, we find that, in the case of $k_0 \gg 1$, the effect of the phase shift θ is not obvious before the disappearing of ZB.

For the limit of $k_0 \ll 1$, the modified Bessel function can be expanded as Taylor series $I_1(x) = \frac{x}{2} + \frac{x^3}{16} + \frac{x^5}{384} + O(x^7)$. By keeping only the first linear term, we get

$$\begin{aligned}\langle y(t)\rangle &\approx 2k_0 e^{-k_0^2}\int_0^\infty d\rho e^{-\rho^2}\rho\cos(t\rho)\\ &= k_0 e^{-k_0^2}\left[1 - tD\left(\frac{t}{2}\right)\right],\end{aligned} \tag{10}$$

where $D(x) = \frac{1}{2}\int_0^\infty e^{-t^2/4}\sin(xt)dt$ is the Dawson function.

We can see from Eq. (10) that there will be no integrated ZB oscillation when the average momentum is very small [see also panel (b) in Fig. 1]. We notice that a similar result is found in 4×4 Luttiger Hamiltonian by Demikhovskii *et al.* [35].

From the above approximate formulas, the amplitude of ZB oscillation $y(t = 0)$ can be obtained for the two limit case. In the case of the average momentum $k_0 \ll 1$, it is proportional to the average momentum. When $k_0 \gg 1$, the ZB amplitude is inversely proportional to the average momentum k_0 (It is worthwhile to notice that the amplitude of ZB in three-component atoms is twice as large as that in two-component atoms [33]). We numerically investigate the amplitude as a function of the average momentum in panel (a) of Fig. 1. In panel (a), there exists a maximum value of the amplitude on the curve. The maximum value occurs at around $k_0 \sim 1$.

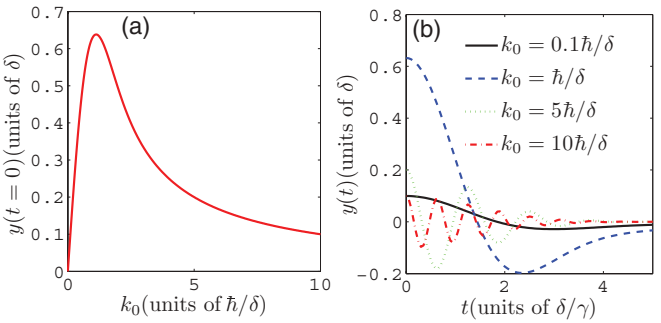

FIG. 1. (Color online) (a) The amplitude of the ZB oscillation as a function of the momentum k_0 under zero Zeeman field. (b) The ZB oscillations under zero Zeeman field for various momentum k_0.

B. The *Zitterbewegung* under the linear Zeeman field ($p \neq 0$ and $q = 0$)

The oscillatory part of $y(t)$ in the Heisenberg picture is

$$(y(t))_{1,1} = \frac{p_x}{p_x^2 + p_y^2 + p^2}\cos\left(t\sqrt{p_x^2 + p_y^2 + p^2}\right). \tag{11}$$

In principle, one could be able to get a asymptotic result though a similar calculations as the case of zero Zeeman field. However, the resulting expression is so long and cumbersome that we could not get clear physical meaning from it. Inspired by the case of zero Zeeman field, we give approximate expression to fit the data obtained from the exact numerical integral under conditions of $k_0 \gg 1$. The approximate formula is

$$\begin{aligned}\langle y(t)\rangle &= \langle g|y(t)|g\rangle\\ &= 2e^{-k_0^2}\mathrm{Re}\left[\int_0^\infty d\rho \frac{\rho^2 e^{-\rho^2 + It\sqrt{\rho^2+p^2}}}{\rho^2 + p^2} I_1(2k_0\rho)\right]\\ &\approx \frac{k_0^2}{k_0^2 + p^2}\frac{e^{-\frac{v_{12}^2 t^2}{4}}}{\left(k_0^4 + \frac{k_0^2 v_{12}^2 t^2}{4}\right)^{\frac{1}{4}}}\cos(\omega_{12}t),\end{aligned} \tag{12}$$

where $v_{12} = \partial_{p_x}\omega_{12}|_{k_0} = k_0/\sqrt{k_0^2 + p^2}$ is the relative group velocity at the average momentum and $\omega_{12} = \sqrt{k_0^2 + p^2}$ is the energy difference between different energy branches at the average momentum. We can see from Eq. (12) that the amplitude is suppressed by the applied linear Zeeman field. With the increase of the linear Zeeman field, the decaying trend is suppressed. The reason is that with the increase of linear Zeeman field, the relative velocity between subpackets corresponding to different energy branches at the average momentum $v_{12} = k_0/\sqrt{k_0^2 + p^2}$ gets smaller. Then, the sustained coherence between subpackets lead to the suppression of decaying. For some specific parameters, we depict the ZB oscillations with only the linear Zeeman field in Fig. 2.

C. The *Zitterbewegung* under the quadratic Zeeman field ($p = 0$ and $q \neq 0$)

The oscillatory part $y(t)_{1,1}$of the position operator in the Heisenberg picture is

$$y(t)_{1,1} = \frac{p_x\omega_{23}\cos(t\omega_{12})}{2\omega_{13}\left(p_x^2 + p_y^2\right)} + \frac{p_x\omega_{12}\cos(t\omega_{23})}{2\omega_{13}\left(p_x^2 + p_y^2\right)}, \tag{13}$$

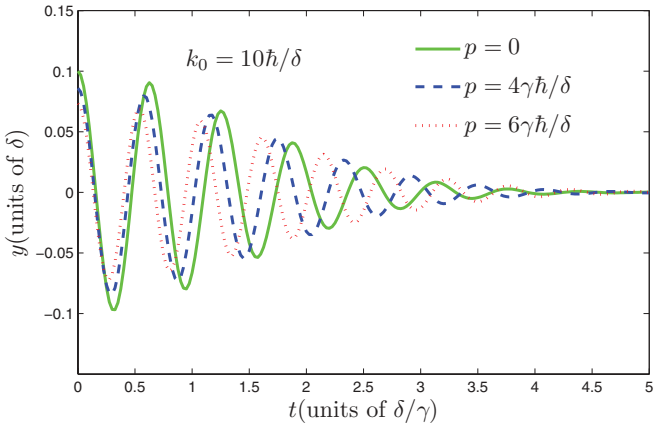

FIG. 2. (Color online) *Zitterbewegung* oscillation in spin-1 atoms under the linear Zeeman field. The ZB oscillation under zero Zeeman field is plotted in the solid green line. The dashed blue and dotted red lines are ZB oscillation under a linear Zeeman field $p = 4\gamma\hbar/\delta$ and $p = 6\gamma\hbar/\delta$, respectively.

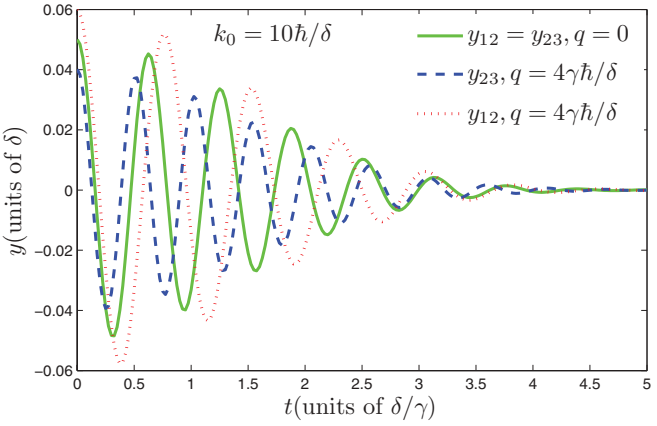

FIG. 3. (Color online) *Zitterbewegung* oscillation under the quadratic Zeeman field. The dashed blue and dotted red lines are ZB oscillations corresponding to ω_{23} and ω_{12} for a quadratic Zeeman field parameter $q = 4\gamma\hbar/\delta$. For the sake of comparison, the solid green line corresponding to zero Zeeman field is also plotted.

where $\omega_{23} = \frac{1}{2}(q + \sqrt{4(p_x^2 + p_y^2) + q^2})$, $\omega_{12} = \frac{1}{2}(-q + \sqrt{4(p_x^2 + p_y^2) + q^2})$, $\omega_{13} = \sqrt{4(p_x^2 + p_y^2) + q^2}$.

By using the similar approximation, the average position along the y direction is approximated by

$$\begin{aligned}\langle y(t)\rangle &= \langle g|y(t)|g\rangle = y_{12} + y_{23} \\ &\approx \frac{\omega_{2,3}(k_0)}{2\omega_{13}} \frac{e^{-\frac{v_{12}^2 t^2}{4}}}{\left(k_0^4 + \frac{k_0^2 v_{12}^2 t^2}{4}\right)^{\frac{1}{4}}} \cos(\omega_{12} t) \\ &\quad + \frac{\omega_{12}(k_0)}{2\omega_{13}} \frac{e^{-\frac{v_{23}^2 t^2}{4}}}{\left(k_0^4 + \frac{k_0^2 v_{23}^2 t^2}{4}\right)^{\frac{1}{4}}} \cos(\omega_{23} t), \end{aligned} \quad (14)$$

where y_{ij} is the ZB oscillation with frequency which is energy difference ω_{ij} between the energy branches i and j at the average momentum. $v_{12} = \partial_{p_x}\omega_{12}|_{k=k_0} = k_0/\sqrt{k_0^2 + q^2}$, $v_{23} = \partial_{p_x}\omega_{23}|_{k=k_0} = k_0/\sqrt{k_0^2 + q^2}$ are relative group velocities between different energy branches at the average momentum.

In the presence of only the quadratic Zeeman field, the ZB oscillation split into two oscillations with different amplitudes and frequencies (see also Fig. 3). The amplitude of the ZB oscillation with higher frequency is smaller than the other one. Because of the equal relative group velocities at the average momentum $v_{12} = v_{23}$, the two ZB oscillations have the same exponential decreasing factor and the decaying trends for the two ZB oscillations are the same on the whole. With the increase of the quadratic Zeeman field, the splitting of both the amplitudes and frequencies between the two ZB oscillations gets more evident.

D. The *Zitterbewegung* under both the linear and the quadratic Zeeman fields ($p \neq 0$ and $q \neq 0$)

In the presence of both the linear and the quadratic Zeeman fields, the analytical expression of the position operator in the Heisenberg picture is quite long and cumbersome. We depict the ZB oscillations with some specific parameters, e.g., $p = 1$, $q = 1$, and $k_0 = 0.87$ in Fig. 4. We can see that there are usually three frequencies when both the linear and the quadratic Zeeman fields exist. We find that when the relative group velocity $v_{ij} = \partial_{p_x}\omega_{ij}|_{k_0}$ between different eigenstates at the average momentum approaches zero, the mean position will damp much more slowly. As shown in the bottom panel of Fig. 4, when the average momentum k_0 is chosen near the elliptic region and the relative velocity between subpackets

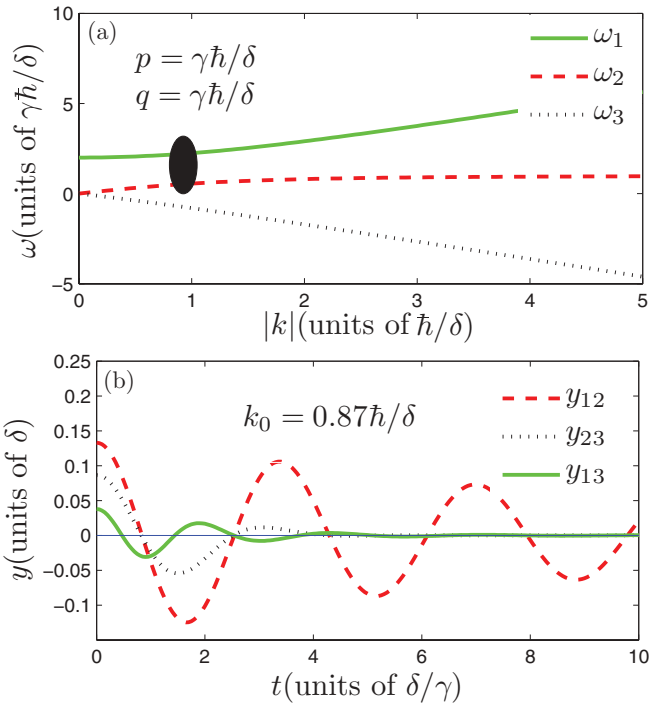

FIG. 4. (Color online) (a) The energy spectrum under both the linear and the quadratic Zeeman fields ($p = \gamma\hbar/\delta$, $q = \gamma\hbar/\delta$). The solid green, dashed red, and dotted black lines denote the three energy branches ω_1, ω_2, and ω_3, respectively. The black elliptic area is the region where the relative group velocity v_{12} approaches zero. (b) The ZB oscillations for the momentum $k_0 = 0.87\hbar/\delta$. The dashed red, dotted black, and solid green lines denote the ZB oscillations with the frequency corresponding to ω_{12}, ω_{23}, and ω_{13}, respectively.

nearly vanishes, the decaying trend of the ZB oscillation corresponding to ω_{12} is suppressed greatly compared with the two others. The scenario of slowing down damping of the ZB oscillation could not occur in two-component atoms due to the limitation of its relative simple energy spectrum. The slowly damping amplitude may be favorable to the observation of ZB in experiments.

III. THE *ZITTERBEWEGUNG* EFFECT IN HARMONIC TRAP

As shown in the above section, the amplitude of ZB oscillation in free space usually decays with time. In the trapped system, the oscillatory behaviors have unique characteristics compared with that in free space. First, due to the confinement of trap, the atoms could not escape from the trap. Hence, the subpackets corresponding to different eigenenergies would always keep coherent, resulting in nondecaying ZB oscillations. Second, due to the existence of infinite energy levels in the trap, the ZB oscillation shows very complicated features.

In this section, we adopt the natural units for harmonic oscillators. The length, mass, and time are measured by $\sqrt{\hbar/M\omega}$, m, and $1/\omega$, respectively. The other physical quantities, such as energy, momentum, and velocity are measured by $\hbar\omega$, $\sqrt{\hbar M\omega}$, and $\sqrt{\hbar\omega/M}$, respectively.

Similar to that in Ref. [31], we decompose the time evolution operator as $U = e^{-iHt} = \sum_l e^{-iE_l t}|l\rangle\langle l|$, where $|l\rangle$ is the eigenstates of Hamiltonian and E_l the corresponding eigenenergy. We generalize Eq. (3) to the trapped system and obtain the position operator in Heisenberg picture as

$$\vec{r}(t) = \vec{r}(0) + \sum_k Z_{k;k} + \sum_{k,l\neq k} e^{i\omega_{kl}t}\vec{Z}_{k;l}, \tag{15}$$

where $\vec{Z}_{k;l} = |k\rangle\langle k|\vec{r}|l\rangle\langle l|$ is the so-called ZB amplitude operator and ω_{kl} is energy difference between eigenenergies. To calculate the average value of position operator, the eigenstates and eigenenergies are required. Before the numerical calculation of the eigenequations, we discuss the symmetries of Hamiltonian. The Hamiltonian have rotational symmetries along z axial direction. Thus, the total angular momenta along z direction $J_z = L_z + F_z$ is a good quantum number. We label the eigenstates and energies with good quantum number $j_z = m$. In the polar coordinates (ρ,θ), the eigenfunction can be written in the following form:

$$|\psi_m(\rho,\theta)\rangle = \begin{pmatrix} \phi_1(\rho)\frac{e^{i(m-1)\theta}}{\sqrt{2\pi}} \\ \phi_0(\rho)\frac{e^{im\theta}}{\sqrt{2\pi}} \\ \phi_{-1}(\rho)\frac{e^{i(m+1)\theta}}{\sqrt{2\pi}} \end{pmatrix}, \tag{16}$$

with $j_z = m$.

In addition to the rotational symmetry, there is time-reversal symmetry in the absence of the Zeeman field. The time-reversal operator is expressed as $T = UK$, with $U = \exp(-i\pi F_y)$ and K the complex conjugate operation. Its matrix form is

$$T = \begin{pmatrix} 0 & 0 & 1 \\ 0 & -1 & 0 \\ 1 & 0 & 0 \end{pmatrix} K. \tag{17}$$

Then the time-reversal state can be obtained as $|\psi_{-m}(\rho,\theta)\rangle = T|\psi_m(\rho,\theta)\rangle$ with degenerate eigenenergies $E_{-m,l} = E_{m,l}$. The eigenstates are doubly degenerate except for the states corresponding to $m = 0$.

We work with the basis of two-dimensional (2D) harmonic oscillator, and the basis can also be introduced by two independent operators in terms of operators of $a_{x(y)}$ [36],

$$\begin{aligned} a_d &= \frac{1}{\sqrt{2}}(a_x - ia_y), \\ a_g &= \frac{1}{\sqrt{2}}(a_x + ia_y), \end{aligned} \tag{18}$$

where $a_{x(y)}$ is annihilation operators of the $x(y)$ direction. The position and momentum operators can be expressed in terms of the operators in Eq. (18) and their corresponding adjoint operators. For example, the y component of the position is $y = \frac{i}{2}(a_d - a_d^\dagger - a_g + a_g^\dagger)$. The harmonic oscillator basis can be written as

$$\left|\chi_{n_d,n_g}\right\rangle = \frac{1}{\sqrt{(n_d)!(n_g)!}}(a_d^\dagger)^{n_d}(a_g^\dagger)^{n_g}|0,0\rangle, \tag{19}$$

where $|0,0\rangle$ is the ground state of a 2D harmonic oscillator. The 2D harmonic oscillator basis can be expressed in the coordinate space as

$$\phi_{n,m}(\rho,\theta) = \left\langle\vec{r}\middle|\chi_{n_d,n_g}\right\rangle = R_{n,m}(\rho)\frac{e^{im\theta}}{\sqrt{2\pi}}, \tag{20}$$

where $n = n_g$, $m = n_d - n_g$, $R_{n,m}(\rho) = (-1)^n\sqrt{\frac{2(n!)}{(n+|m|)!}}\rho^{|m|}e^{-\frac{\rho^2}{2}}L_n^{|m|}(\rho^2)$, $L_n^{|m|}(x) = \Sigma_{k=0}^n C_{n+|m|}^{n-k}\frac{(-x)^k}{k!}$ is the associated Laguerre polynomial and $C_n^k = \frac{n!}{(n-k)!k!}$ is the binomial coefficient.

From the expression of the position operators in terms of $a_{g(d)}$ and their adjoint operators, there exist an important selection rule for ZB amplitude operators

$$\begin{aligned} \vec{Z}_{m,l;m',l'} &= |m,l\rangle\langle m,l|\vec{r}|m',l'\rangle\langle m',l'| = 0, \\ &(m - m' \neq \pm 1), \end{aligned} \tag{21}$$

where l labels the eigenstates belonging to the same quantum m. It is shown that only for $m = m' \pm 1$, there exist nonvanishing ZB amplitude. From the above equation, it is found that the second term in Eq. (15) vanishes, i.e., $\vec{Z}_{k;k} = \vec{Z}_{m,l;m,l} = 0$.

One can express the Hamiltonian in the form of a matrix by adopting the harmonic oscillator basis. The corresponding eigenenergies and eigenstates can be obtained through direct numerical diagonalization [37].

Now we investigate the ZB oscillatory characteristics in the trap. First of all, as shown by Eq. (15), when the the initial state is the superposition of two eigenstates, there would be an oscillation with one single frequency which is the difference of two eigenenergies. The amplitude of the oscillation does not decay. This is because the components corresponding to two eigenenergies in the initial state always keep coherent in the trap, as stated before.

Next, we calculated the ZB oscillations when an Gaussian wave packet with nonvanishing average momentum is used as an initial state. The projections of the initial state onto the

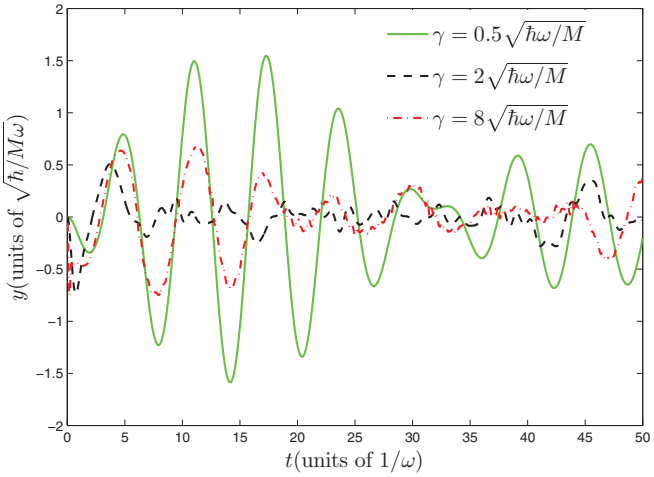

FIG. 5. (Color online) The ZB oscillations with a Gaussian wave packet as an initial state in the trap for the wave packet width $\delta = \sqrt{\hbar/M\omega}$ and the momentum $k_0 = 2\sqrt{\hbar M\omega}$. The solid green, dashed black, and red dash-dotted lines correspond to the spin-orbit coupling strengths $\gamma = 0.5\sqrt{\hbar\omega/M}$, $2\sqrt{\hbar\omega/M}$, and $8\sqrt{\hbar\omega/M}$, respectively.

harmonic basis are required in the calculation the average value of the position. The detailed calculations of the projection are listed in the Appendix. From Eq. (15), we know that the number of the frequencies of the oscillation involved in ZB oscillation is usually arbitrary when the initial state is chosen in a completely arbitrary fashion. Using the Gaussian wave packet as the initial state, we find that there are indeed a lot of frequencies in the ZB oscillation.

For some specific parameters, the ZB oscillations in the trap are shown in Fig. 5. From Fig. 5, we can see that, for both the weak and strong spin-orbit coupling, the ZB oscillations display the harmonic oscillator characteristics within short time interval (20 time units in Fig. 5). This is because when the spin-orbit coupling approaches zero, the energy-spectrum approaches the harmonic oscillator spectrum. In the case of the strong spin-orbit limit, the eigenenergies can be approximated by $E_{m,n} = [-\gamma^2 + 2n + 1 + m^2/\gamma^2]/2$, which is analogous to the energy spectrum formula of two-component atoms with strong spin-orbit coupling and harmonic trap [22,38]. Compared with the two-components atoms, the ground state is not degenerate. The energy spectrum in strong spin-orbit coupling limit form landau level-like spectrum. Thus, in cases of both weak and strong spin-orbit coupling limit, the energy level spacing approaches $\hbar\omega$. With the increase of the time, the out-of-phase oscillations begin to appear. Meanwhile, the oscillations with high-frequency begin to manifest themselves (see the red dash-dotted line in Fig. 5).

In the presence of the intermediate-strength spin-orbit coupling, the ZB shows quite complicatedly and irregularly oscillatory characteristics. It is due to the complicated energy spectrum and coexistence of oscillations with various frequencies in ZB.

We explore the ZB oscillation in the presence of both the Zeeman field and the harmonic trap. For the weak spin-orbit coupling, the top panel in Fig. 6 shows that the ZB effect is manifested as beat oscillation. The beat period gets larger and larger with the increase of the linear Zeeman field. The

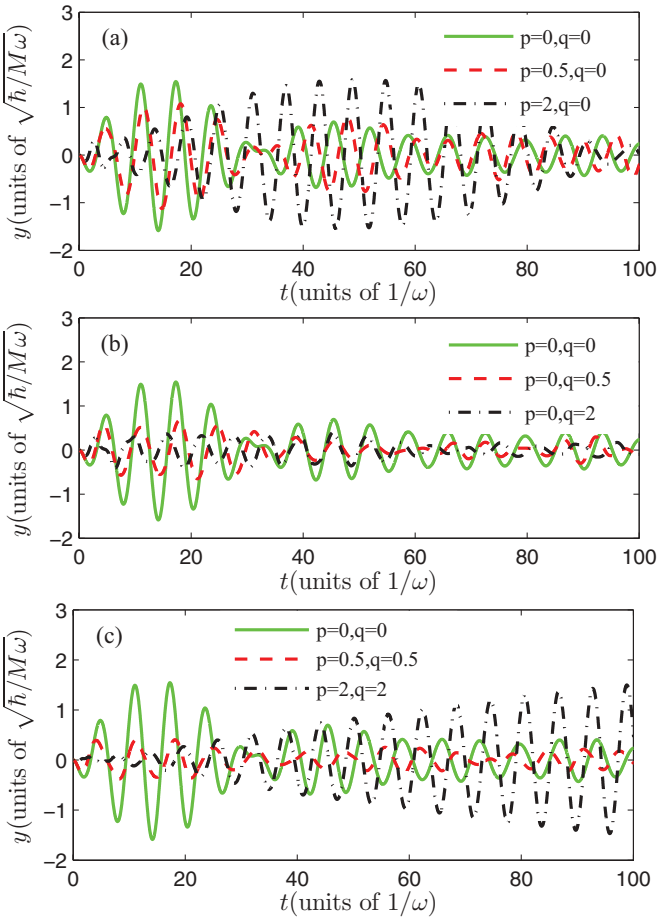

FIG. 6. (Color online) The ZB oscillations in the presence of both the harmonic trap and the Zeeman field with the wave packet width $\delta = \sqrt{\hbar/M\omega}$, the average momentum $k_0 = 2\sqrt{\hbar M\omega}$, and the spin-orbit coupling strength $\gamma = 0.5\sqrt{\hbar\omega/M}$, respectively. The solid green, dashed red, and black dash-dotted lines correspond to the ZB oscillations for various Zeeman parameters (the unit of the Zeeman parameters p and q is $\hbar\omega$).

quadratic Zeeman field usually suppresses the amplitude of the ZB oscillation, as shown by the the middle panel in Fig. 6. In the presence of both the linear and the quadratic Zeeman fields, we can see that the beat period gets even much larger compared with the case where only the linear Zeeman field is included, as shown in the bottom panel in Fig. 6 (see the black dash-dotted lines). For strong spin-orbit coupling, the amplitude of the ZB oscillation is usually smaller than that of weak spin-orbit coupling as shown in Fig. 7. At the same time the high-frequency oscillations are manifested more evidently.

IV. EFFECT OF INTERACTION ON THE *ZITTERBEWEGUNG* OSCILLATION

In this section, we numerically simulate the dynamical evolution of the spin-orbit-coupled ^{23}Na atoms by solving the corresponding GP equation. Taking the axial trap frequency $\omega_z = 2\pi \times 800$ Hz, the transverse trap frequency $\omega_\perp = 2\pi \times 90$ Hz, the total number of atoms $N = 10^4$, and the experimental values of scattering length of ^{23}Na atoms $a_0 = 46a_B$, $a_2 = 52a_B$ (a_B is the Bohr radius), the corresponding

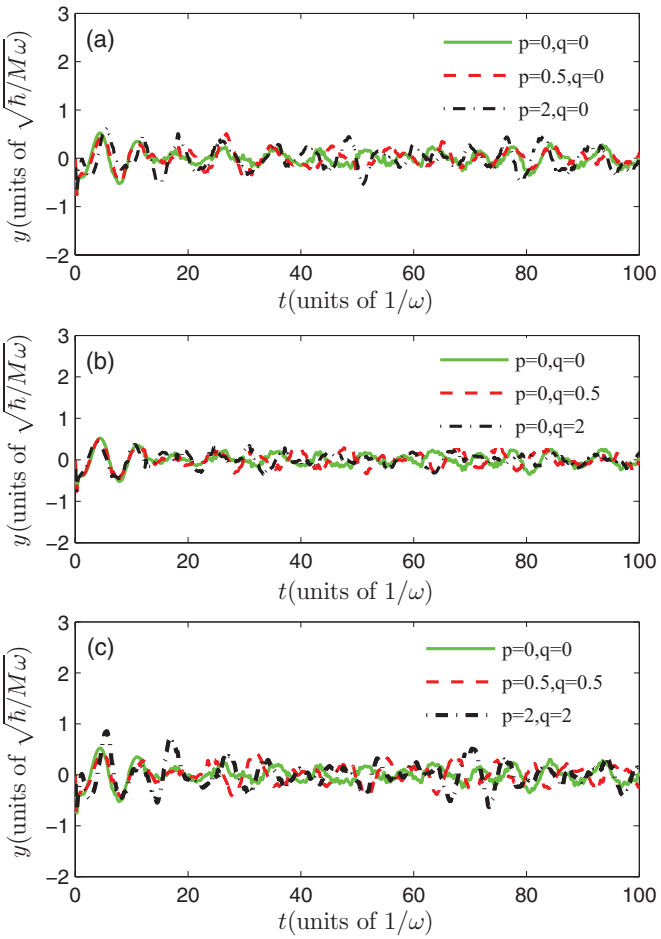

FIG. 7. (Color online) The ZB oscillations in the presence of both the harmonic trap and the Zeeman field with the wave-packet width $\delta = \sqrt{\hbar/M\omega}$, the average momentum $k_0 = 2\sqrt{\hbar M\omega}$, and the spin-orbit coupling strength $\gamma = 5\sqrt{\hbar\omega/M}$, respectively (the unit of the Zeeman parameters p and q is $\hbar\omega$).

two dimensionless interaction parameters $c_0 = 178.90$ and $c_2 = 7.16$ (in natural units of harmonic oscillator). The effect of interaction on the ZB oscillation in the trap is considered in Fig. 8. Comparing it with Fig. 5 (without interaction), the beat oscillation period get longer for weak spin-orbit coupling. For intermediate and strong spin-orbit coupling strength, the oscillatory amplitude for a long time is slightly suppressed. Even though the ZB effect originates from the single-particle Hamiltonian, it is still robust in the presence of interaction between atoms. Therefore, the ZB oscillation is a universal phenomenon in the dynamical evolution of the spin-orbit-coupled atoms.

In this paragraph, we discuss the experimental aspects on the ZB oscillation. The ZB oscillation is accompanied by a damped oscillation of the probability density with time for each component [34]. The oscillatory properties of position operator, such as the decaying trend and the oscillatory frequency, e.g., can be reflected by the damped oscillation of the number of atoms. The oscillation of the number can be obtained through a series of time-of-flight measurement for various values of time [17]. Nevertheless, one also could use nondestructive phase-contrast imaging technique to directly

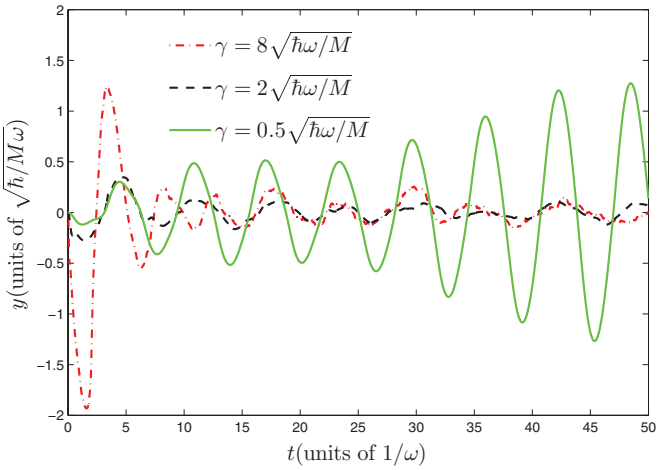

FIG. 8. (Color online) The ZB oscillations in the presence of the both harmonic trap and the interaction between atoms with the wave-packet width $\delta = \sqrt{\hbar/M\omega}$ and the momentum $k_0 = 2\sqrt{\hbar M\omega}$, respectively.

observe the atoms *in situ* [39–41]. The phase-contrast imaging is very suitable to observe the evolution of optical dense condensate in trap. The information of the density distribution of atoms can be extracted from the resulting image. The magnitude of the ZB in ultracold atoms can be evaluated through some typical experimental parameters. Taking ^{23}Na atoms, for example, one can adopt the experiment parameters, such as the wavelength of Raman laser $\lambda \sim 600$ nm and the angle between two Raman beams $\theta = \pi/2$, which corresponds to a spin-orbit strength $\gamma = \sqrt{2}\pi\hbar/(M\lambda) \approx 1.93$ cm/s ($M = 3.82 \times 10^{-26}$ kg for ^{23}Na). Applying a magnetic field of $B = 450$ mG, the resulting quadratic Zeeman parameter $q \sim h \times 56$ Hz. The effective linear Zeeman parameter p can be tuned to the same order of the quadratic Zeeman parameter through the frequency difference between Raman lasers. One can prepare a condensate of the total atoms number $N = 10^4$ in a harmonic trap with z axial trapping frequency $\omega_z = 2\pi \times 439$ Hz and radial trapping frequency $\omega_\perp = 2\pi \times 1.57$ Hz. The BEC has a pancakelike shape with z axial characteristic length $a_z \sim 1$ μm and radial wave packet width $\delta \sim 50$ μm. Under the condition of the above parameters, the interaction between atoms and the potential of the harmonic trap ($\sim h \times 7$ Hz) are much smaller than the spin-orbit coupling interaction energy $\gamma\hbar/\delta \sim q \sim h \times 56$ Hz. The amplitude of ZB can be as large as one-half of the wave packet width δ as shown in Fig. 1 in Sec. II. The above parameters are accessible in cold-atom experiments.

V. SUMMARY

In summary, we have investigated the ZB effect in spin-1 atoms in the presence of the Zeeman field and the external harmonic trap. It is shown that the ZB oscillations could be greatly affected by the external Zeeman field and the trap. The external Zeeman field could suppress or enhance the ZB amplitude and change the frequencies of oscillation. In addition, multifrequency oscillations could appear in the presence of the Zeeman field. Through adjusting both the linear and the quadratic Zeeman fields properly, we could

obtain a much slower damping ZB oscillation in the spin-1 ultracold atoms. In the presence of a harmonic trap, there would be the ZB oscillation without damping and with arbitrary number of frequencies. The ZB in the trap displays very complicated and irregular oscillation characteristics due to its complicated energy spectrum. Furthermore, it is shown that the ZB oscillation is robust even in the presence of interaction between atoms.

The present work should help us understand the roles of external Zeeman field and trap in the ZB oscillations. The investigation of the effects induced by the external field and trap on ZB oscillation opens up new possibilities for the manipulation and control of the ZB oscillation. We anticipate the ZB effect will be detected in the widely studied cold-atom experiments with spin-orbit coupling interactions.

ACKNOWLEDGMENTS

This work was supported by the NKBRSFC under Grants No. 2011CB921502, No. 2012CB821305, No. 2009CB930701, and No. 2010CB922904, NSFC under Grants No. 10934010, No. 11228409, No. 61227902, and No. 11247206, and NSFC-RGC under Grants No. 11061160490 and No. 1386-N-HKU748/10.

APPENDIX: THE PROJECTIONS OF THE GAUSSIAN PACKET ONTO THE HARMONIC OSCILLATOR BASIS

In this Appendix, we give the calculation of the projections of the initial Gaussian wave packet onto the harmonic oscillator basis, which is required in the calculation of the average values of the position operator. The initial wave packet reads

$$|g\rangle = \frac{1}{\sqrt{\pi\delta^2}} e^{-\frac{(x^2+y^2)}{2\delta^2}} e^{ik_0 x}, \tag{A1}$$

where δ denotes the width of the wave packet and k_0 is the average momentum of the wave packet.

The projection onto the harmonic oscillator basis is

$$\langle \phi_{n,m}|g\rangle = \frac{2(-1)^n i^{|m|}}{\delta}\sqrt{\frac{n!}{(n+|m|)!}} \times \int_0^{+\infty} \rho^{|m|+1} e^{-\sigma^2\rho^2} L_n^{|m|}(\rho^2) J_{|m|}(k_0\rho)d\rho, \tag{A2}$$

where $|\phi_{n,m}\rangle = R_{n,m}(\rho)\frac{e^{im\theta}}{\sqrt{2\pi}}$, $\sigma^2 = \frac{1}{2}(1+\frac{1}{\delta^2})$, and $J_{|m|}(x)$ is the Bessel functions of order $|m|$.

The associated Laguerre polynomial consists of various monomials. The integrals corresponding to the monomials can be obtained through an integral identity

$$\int_0^{+\infty} \rho^{\mu-1} e^{-p^2\rho^2} J_\nu(a\rho)d\rho = \frac{\Gamma\left(\frac{\mu+\nu}{2}\right)}{2p^\mu\Gamma(\nu+1)}\left(\frac{a}{2p}\right)^\nu e^{-\frac{a^2}{4p^2}} {}_1F_1\left(\frac{\nu-\mu}{2}+1;\nu+1;\frac{a^2}{4p^2}\right), \tag{A3}$$

where $\Gamma(z)$ is Euler's Γ function and ${}_1F_1(\alpha;\beta;x)$ is the generalized hypergeometric functions [42]. Combining Eq. (A2) with Eq. (A3), we can obtain the projections by summing up all integral values corresponding to the monomials. The ZB amplitude operators $\vec{Z}_{k;l}$ in Eq. (15) are also calculated within the harmonic oscillator basis and the mean value of the position operator can be obtained correspondingly.

[1] E. Schrödinger, Sitzungsber. Preuss. Akad. Wiss. Phys.-Math. Kl. **24**, 418 (1930).
[2] T. M. Rusin and W. Zawadzki, Phys. Rev. B **80**, 045416 (2009).
[3] J. Schliemann, D. Loss, and R. M. Westervelt, Phys. Rev. Lett. **94**, 206801 (2005).
[4] J. Cserti and G. Dávid, Phys. Rev. B **74**, 172305 (2006).
[5] X. D. Zhang, Phys. Rev. Lett. **100**, 113903 (2008).
[6] L. Lamata, J. León, T. Schätz, and E. Solano, Phys. Rev. Lett. **98**, 253005 (2007).
[7] R. Gerritsma, G. Kirchmair, F. Zähringer, E. Solano, R. Blatt, and C. F. Roos, Nature (London) **463**, 68 (2010).
[8] J. Schliemann, New J. Phys. **10**, 043924 (2008).
[9] Z. F. Jiang, R. D. Li, S. C. Zhang, and W. M. Liu, Phys. Rev. B **72**, 045201 (2005).
[10] S. Q. Shen, Phys. Rev. Lett. **95**, 187203 (2005).
[11] R. Winkler, U. Zülicke, and J. Bolte, Phys. Rev. B **75**, 205314 (2007).
[12] M. Lee and C. Bruder, Phys. Rev. B **72**, 045353 (2005).
[13] Z. Y. Wang and C. D. Xiong, Phys. Rev. A **77**, 045402 (2008).
[14] Y. J. Lin, K. J. García, and I. B. Spielman, Nature (London) **471**, 83 (2011).
[15] L. W. Cheuk, A. T. Sommer, Z. Hadzibabic, T. Yefsah, W. S. Bakr, and M. W. Zwierlein, Phys. Rev. Lett. **109**, 095302 (2012).
[16] Y. J. Lin, R. L. Compton, A. R. Perry, W. D. Phillips, J. V. Porto, and I. B. Spielman, Phys. Rev. Lett. **102**, 130401 (2009).
[17] P. J. Wang, Z. Q. Yu, Z. K. Fu, J. Miao, L. H. Huang, S. J. Chai, H. Zhai, and J. Zhang, Phys. Rev. Lett. **109**, 095301 (2012).
[18] G. Juzeliūnas, J. Ruseckas, and J. Dalibard, Phys. Rev. A **81**, 053403 (2010).
[19] C. Wang, C. Gao, C. M. Jian, and H. Zhai, Phys. Rev. Lett. **105**, 160403 (2010).
[20] T. L. Ho and S. Zhang, Phys. Rev. Lett. **107**, 150403 (2011).
[21] S.-K. Yip, Phys. Rev. A **83**, 043616 (2011).
[22] H. Hu, B. Ramachandhran, H. Pu, and X. J. Liu, Phys. Rev. Lett. **108**, 010402 (2012).
[23] S. Sinha, R. Nath, and L. Santos, Phys. Rev. Lett. **107**, 270401 (2011).
[24] X. Q. Xu and J. H. Han, Phys. Rev. Lett. **107**, 200401 (2011).
[25] X. F. Zhou, J. Zhou, and C. J. Wu, Phys. Rev. A **84**, 063624 (2011).
[26] S.-W. Su, I.-K. Liu, Y.-C. Tsai, W. M. Liu, and S.-C. Gou, Phys. Rev. A **86**, 023601 (2012).
[27] J. Y. Vaishnav and C. W. Clark, Phys. Rev. Lett. **100**, 153002 (2008).
[28] Q. Zhang, J. Gong, and C. H. Oh, Phys. Rev. A **81**, 023608 (2010).

[29] D. W. Zhang, Z. D. Wang, and S. L. Zhu, Front. Phys. **7**(1), 31 (2012).
[30] M. Merkl, F. E. Zimmer, G. Juzeliūnas, and P. Öhberg, Europhys. Lett. **83**, 54002 (2008).
[31] G. Dávid and J. Cserti, Phys. Rev. B **81**, 121417 (2010).
[32] M. Ueda, *Fundamentals and New Frontiers of Bose-Einstein Condensation* (World Scientific, Singapore, 2010).
[33] V. Y. Demikhovskii, G. M. Maksimova, and E. V. Frolova, Phys. Rev. B **78**, 115401 (2008).
[34] T. M. Rusin and W. Zawadzki, Phys. Rev. B **76**, 195439 (2007).
[35] V. Y. Demikhovskii, G. M. Maksimova, and E. V. Frolova, Phys. Rev. B **81**, 115206 (2010).
[36] C. C. Tannoudji, B. Diu, and F. Laloë, *Quantum Mechanics*, Vol. I (Hermann and John Wiley & Sons, Paris, 1977).
[37] B. Ramachandhran, B. Opanchuk, X. J. Liu, H. Pu, P. D. Drummond, and H. Hu, Phys. Rev. A **85**, 023606 (2012).
[38] C. J. Wu, I. M. Shem, and X. F. Zhou, Chin. Phys. Lett. **28**, 097102 (2011).
[39] M. R. Andrews, M.-O. Mewes, N. J. van Druten, D. S. Durfee, D. M. Kurn, and W. Ketterle, Science **273**, 84 (1996).
[40] J. M. Higbie, L. E. Sadler, S. Inouye, A. P. Chikkatur, S. R. Leslie, K. L. Moore, V. Savalli, and D. M. Stamper-Kurn, Phys. Rev. Lett. **95**, 050401 (2005).
[41] R. Meppelink, R. A. Rozendaal, S. B. Koller, J. M. Vogels, and P. van der Straten, Phys. Rev. A **81**, 053632 (2010).
[42] Z. X. Wang and D. R. Guo, *Special Functions* (World Scientific, Singapore, 1989).